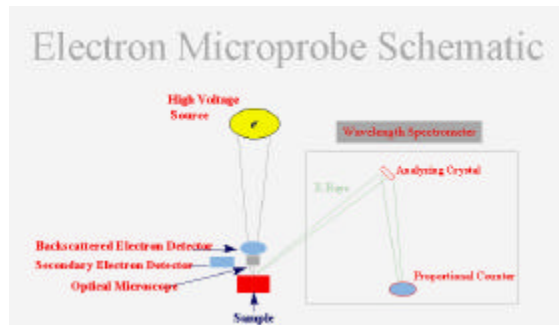


# Electron Probe Microanalysis (EPMA)

By John J. Donovan

(portions from J. I. Goldstein, D. E. Newbury, P. Echlin, D. C. Joy, C. Fiori, E. Lifshin, "Scanning Electron Microscopy and X-Ray Microanalysis", 2nd Ed., Plenum, New York, 1992)

## Overview



(by Michael Schaffer, University of Oregon)

An electron microprobe is an electron microscope designed for the non-destructive x-ray microanalysis and imaging of solid materials. It is essentially a hybrid instrument combining the capabilities of both the scanning electron microscope (SEM) and an x-ray fluorescence spectrometer (XRF), with the added features of fine-spot focusing ( $\sim 1$  micrometer), optical microscope imaging, and precision-automated sample positioning. The analyst makes measurements while observing the sample (with the optical microscope or with a secondary/backscattered electron image) and selecting specific analysis locations (using the precision sample stage).

Related instruments: Scanning Electron Microscope (SEM) and Analytical Electron Microscope (AEM).

The technique is capable of high spatial resolution ( $\sim 1\mu\text{m}$ ) and relatively high analytical sensitivity ( $<0.5\%$  for major elements) and detection limits ( $\sim 100$  ppm for trace elements). It can also acquire digital secondary-electron and backscattered-electron and cathodoluminescence images as well as digital x-ray maps. It is normally equipped with up to 5 wavelength-dispersive spectrometers. They also contain:

- an electron gun (usually a heated tungsten filament) produces the electrons, which are then focused with 2 condenser lenses, filtered through several apertures and finely focused on the specimen (with the objective lens) on the area of interest, (essentially the image of the filament is “de-magnified” by the electron lens system in a manner analogous to the looking through the wrong end of a telescope),
- a high vacuum ( $10^{-6}$  torr) is required, for the life of the filament and to minimize electron dispersion in the column,

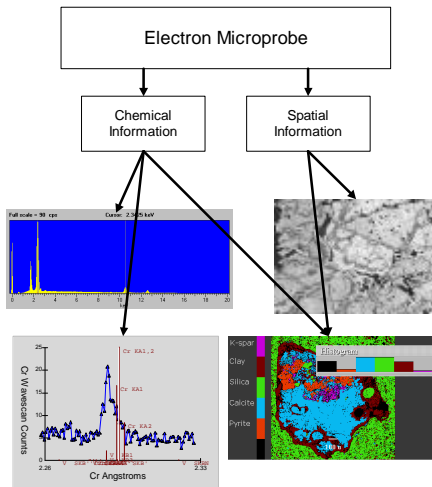
- scanning coils, so the beam can raster across a specimen, producing a scanned image (a la SEM),
- secondary electron detectors (which in scanning mode yield SE images, showing surface features),
- backscattered electron (BSE) detectors yielding images where different phases of differing mean atomic number stand out sharply,
- cathodo-luminescence (CL) detectors, where the light emitted from the electron-specimen interaction can be imaged, and can clearly show features in minerals and semi-conductors that would be difficult to see compositionally (these are features due to differences in specific trace element concentrations, or crystal lattice defects)
- EDS detectors which are mostly used for quick appraisal (qualitative analysis) of the specimen by examining the entire x-ray spectrum, to determine the optimum analytical procedure for use with WDS

Most of the periodic table can in principle be analyzed (Beryllium through Uranium), subject to several important considerations.

#### *Sample Preparation*

The volume sampled is typically a few cubic microns at the surface, corresponding to a weight of a few picograms and are therefore sensitive to surface contamination. Samples should be prepared as clean, flat, polished solid mounts up to 1 inch in diameter or as uncovered petrographic thin-sections, and must be stable in a  $10^{-5}$  torr vacuum environment and under electron bombardment. For best results, samples must be polished to within a 0.05  $\mu\text{m}$  flat surface. After preparation, samples are coated with an approximately 200 Angstrom (10 nm) layer of carbon using a carbon or other conductive material in an evaporator. The use of a sputter coater which produces films of varying thickness is not used in EPMA.

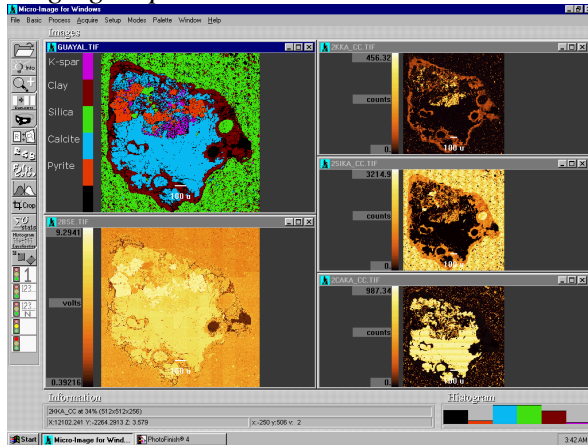
What do we get from EPMA?



### *Quantitative Capabilities*

EPMA is primarily utilized to determine the elemental composition of various materials on a micro scale. The use of standards and matrix corrections can realize accuracies of typically 3-5% or better which allows the determination of many (inorganic) chemical formulas.

### *Imaging Capabilities*



One may also perform digital imaging. The ability to simultaneously acquire wavelength-dispersive and energy-dispersive x-ray maps as well as secondary-electron or backscattered-electron images is often useful for many sample investigations.

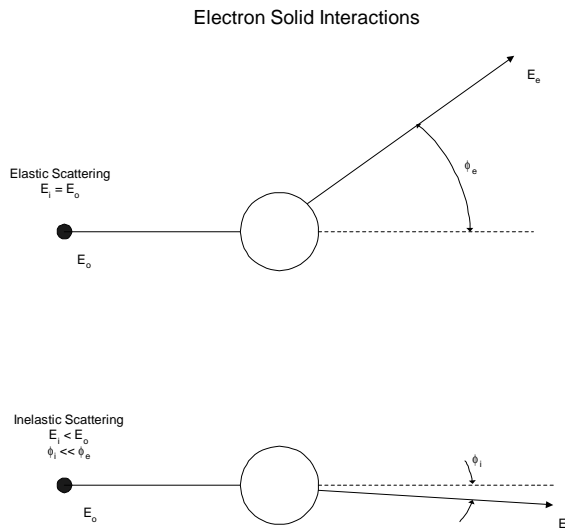
Two basic x-ray mapping modes are available, digital mapping, which is essentially a multiple-scan averaging mode that produces a binary image based on x-ray detection at each pixel (i.e. a noise suppressed dot-mapping technique), and counter-mode mapping, which is a slower pixel-by-pixel map acquisition mode with a user specified dwell time per pixel. The digital mapping and counter-mode mapping modes allow for either relatively fast acquisition with high resolution to discriminate phases with large chemical differences, and slower acquisition with low resolution to discriminate phases with smaller chemical differences, respectively.

### *Electron solid interactions*

The electron beam interacts with the specimen atoms and is significantly scattered by them as opposed to penetrating the sample in a linear fashion.

When an incident electron beam interacts with the atoms in a sample, most of the energy of the electron beam will eventually end up as heat (phonon excitation of the atomic lattice), however before the electrons come to rest they primarily undergo two types of scattering - elastic and inelastic.

### **Electron scattering mechanisms:**



In the former, only the trajectory changes and the kinetic energy and velocity remain essentially constant (due to large differences between the mass of the electron and nucleus), this is known as electron backscattering. In the case of inelastic scattering, the incident electrons will have their trajectories only slightly perturbed but they will lose energy through interactions with the orbital electrons of the atoms in the specimen. These inelastic interactions include phonon excitation (atomic lattice vibrations), plasmon production (free electrons), and also continuum radiation (bremsstrahlung or “braking radiation, Auger (pronounced o-jhay) production (ejection of outer shell electrons), characteristic x-ray radiation and cathodo-luminescence (visible light fluorescence) the last two both from inner orbital electron ionization.

In the electron microprobe, specimens that are “infinitely thick” relative to the scattering of the incident beam are utilized in order to calculate the interaction volume more accurately by assuming that all electrons come to rest inside the specimen.

However, this means that the electrons continue to scatter as they lose energy and may still induce production of characteristic x-rays down to the energy of the lowest energy x-ray being measured. This means that the electron interaction and the x-ray production volume are typically much larger than the size of the incident electron beam.

Since we are typically pushing the resolution of the instrument, it is critical to understand the size of the electron “analytical” volume (that is, the region where the x-ray are emitted from).

The two trends that limit the size and shape of the interaction volume are the energy loss of the electron beam through inelastic interactions and electron loss or backscattering through elastic interactions. Specifically, the electron range is limited by the energy losses and the shape is defined by the high angle scattering of the backscattered electrons.

### *Monte-Carlo modeling*

Several software packages have been developed that model the scattering (elastic and inelastic) of electrons that occurs when they interact with specimens. These programs demonstrate very graphically the extent of elastic scattering that occur in bulk specimens, producing the ~micron-size "interaction volume", which is the spatial resolution of chemical analysis in EMPA.

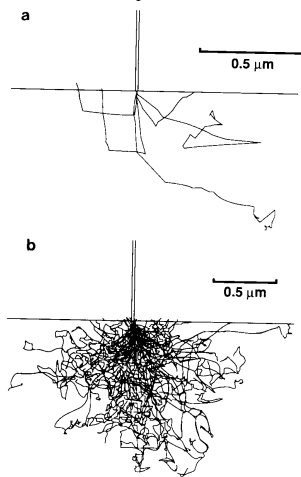


**Figure 3.7.** Monte Carlo electron-trajectory simulation of the beam interaction in iron,  $E_0 = 20$  keV, tilt = 0°. (a) Plot of five trajectories, showing random variations. (b) Plot of 100 trajectories projected on a plane perpendicular to the surface, giving a visual impression of the interaction volume.

from J. I. Goldstein, D. E. Newbury, P. Echlin, D. C. Joy, C. Fiori, E. Lifshin, "Scanning Electron Microscopy and X-Ray Microanalysis", 2nd Ed., Plenum, New York, 1992

Traditionally, textbooks show diagrams of electron scattering in a tear-shaped pattern in the specimen; this is actually a "special case", for a low atomic number plastic -- appropriate for some biological material but not for higher Z materials such as minerals or metals.

### **Interaction volumes versus beam energy**

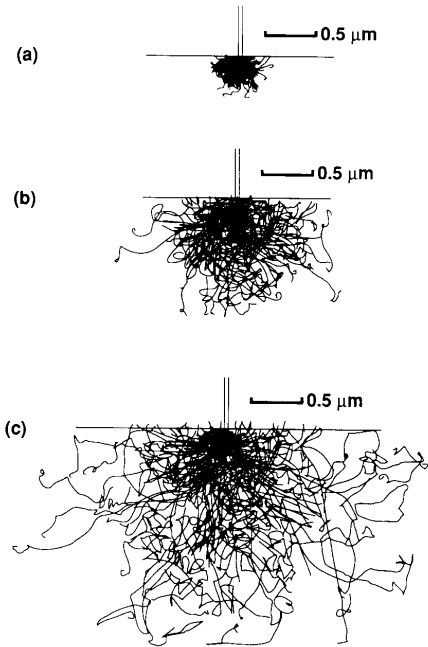


**Figure 3.8.** Monte Carlo electron-trajectory simulations of the interaction volume in iron as a function of beam energy: (a) 10 keV, (b) 20 keV, (c) 30 keV.

from J. I. Goldstein, D. E. Newbury, P. Echlin, D. C. Joy, C. Fiori, E. Lifshin, "Scanning Electron Microscopy and X-Ray Microanalysis", 2nd Ed., Plenum, New York, 1992

## Interaction volumes versus atomic number

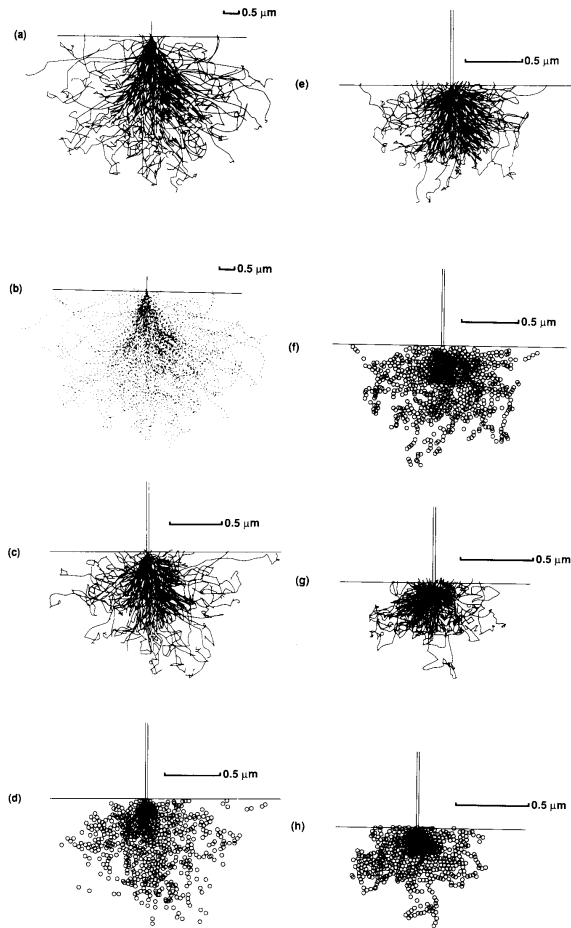


**Figure 3.9.** Monte Carlo electron-trajectory simulations of the interaction volume at 20 keV and  $0^\circ$  tilt in various targets; both trajectory plots and sites of inner-shell ionization are shown: (a), (b) carbon *K*-shell; (c), (d) iron *K*-shell; (e), (f) silver *L*-shell; (g), (h) uranium *M*-shell.

from J. I. Goldstein, D. E. Newbury, P. Echlin, D. C. Joy, C. Fiori, E. Lifshin, "Scanning Electron Microscopy and X-Ray Microanalysis", 2nd Ed., Plenum, New York, 1992

One can model a variety of conditions (sample thickness, accelerating voltage) on a computer prior to using an electron microbeam instrument, to determine, for example, spatial resolution of the x-ray data.

### *X-ray production*

The incident electron beam traveling through the specimen may inelastically interact with the orbital electrons, as mentioned previously, to cause a displacement of the orbital electrons from their shells around nuclei of atoms comprising the sample. This interaction places the atom in an excited (unstable) state, which then seeks to return to a ground or unexcited state.

### **Electron Energy Transition**

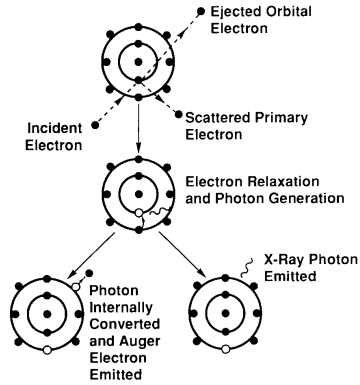


**Figure 3.33.** Schematic illustration of the process of inner-shell ionization and subsequent de-excitation by electron transitions. The difference in energy between the shells is expressed either by the ejection of an energetic electron with characteristic energy (Auger process) or by the emission of a characteristic x ray.

from J. I. Goldstein, D. E. Newbury, P. Echlin, D. C. Joy, C. Fiori, E. Lifshin, "Scanning Electron Microscopy and X-Ray Microanalysis", 2nd Ed., Plenum, New York, 1992

There are two ways for this electron energy transition to occur, one way the energy difference is expressed is by the ejection of outer shell electrons. This is the Auger process. The other way for an atom to return to ground state is for an electron in a higher orbital to "fall" into the vacant shell and take the place of the displaced electron. When this occurs, energy is lost and a single x-ray of a narrow energy range is emitted. This is the production of characteristic x-ray radiation and it is the basis of the technique that we will be discussing.

The electronic orbits of each element are relatively unique and thus the set of x-rays emitted from these electron interactions are also fairly characteristic with respect to the energy or wavelength for each element. Energy and wavelength are related by the equation,

$$I = \frac{12.3985}{E}$$

where wavelength ( $\lambda$ ) is in Angstroms and energy (E) is in keV

### X-ray transition levels

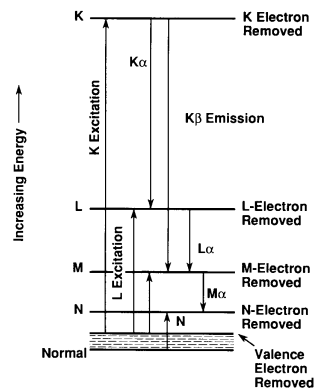


**Figure 3.35.** Energy-level diagram for an atom, illustrating the excitation of the K, L, M, and N shells and the formation of K $\alpha$ , K $\beta$ , L $\alpha$ , and M $\alpha$  x rays.

from J. I. Goldstein, D. E. Newbury, P. Echlin, D. C. Joy, C. Fiori, E. Lifshin, "Scanning Electron Microscopy and X-Ray Microanalysis", 2nd Ed., Plenum, New York, 1992

For example, if an incident electron strikes an inner K shell electron and knocks it out of its orbit, an L shell electron will drop into the K orbit and emit a K alpha x-ray of some diagnostic energy or wavelength; there is a lower probability that an M shell electron will drop in, yielding a K beta x-ray. Similarly, an L shell electron may be displaced by the incident electron and be replaced by an M shell, and in this case emits an L alpha x-ray.

The practical result of this is that because elements of increasing  $Z$  give off a greater variety of x-rays for they have more electrons in a greater number of orbits about their nucleus, that the lower atomic number elements have fewer lines to distribute the probability of interacting with an incident electron and hence their lines are generally are stronger in intensity, and second, the potential overlap of the greater number of peaks from higher atomic number elements constitutes the source of one potential problem in interpreting x-ray spectra.

The generated characteristic x-ray intensity relates to the interaction volume because the size of this interaction volume is directly proportional to the generated x-ray intensity, that is, the greater the number of atoms excited, the greater the generated x-ray intensity, it is essential to know, if not the absolute interaction volume, then the relative interaction volume in materials of various compositions for.

### *X-ray Detection*

By placing a suitable x-ray detector coupled to a set of electronic components (amplifiers, counters, analog-digital converters) and a computer, one can detect and analyze x-rays emitted from a sample undergoing electron bombardment. The resulting x-ray spectrum can be displayed according to energy (Energy Dispersive X-ray Spectroscopy - EDS) or wavelength (Wavelength Dispersive X-ray Spectroscopy -WDS). These data can then be either analyzed to give an indication of which elements occur in a sample (qualitative), or in a much more rigorous process, a precise and accurate (quantitative) chemical analysis.

### *Energy Dispersive X-ray Analysis (EDS)*

X-rays emitted from a sample under electron bombardment are collected with a liquid nitrogen-cooled solid state detector

### **EDS schematic**

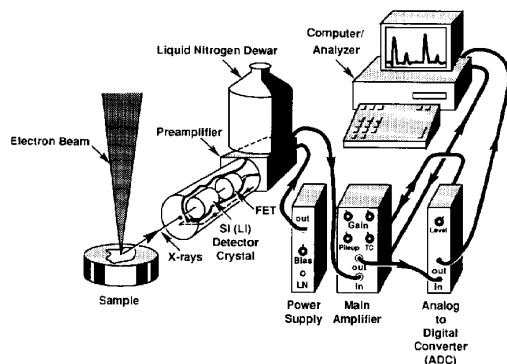
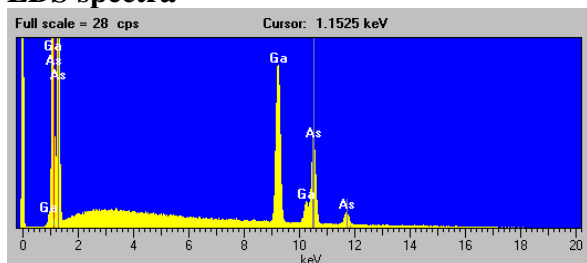


**Figure 5.20.** Schematic representation of an energy-dispersive spectrometer and its associated electronics.

and analyzed via computer according to their energy. Typically, the computer programs used in EDS will display a real time histogram

### EDS spectra



of number of X-rays detected per channel (variable, but usually 10 electron volts/channel) versus energy expressed in keV (thousand electron volts).

In practice, EDS is most often used for qualitative elemental analysis, simply to determine which elements are present and their relative abundance. Depending upon the specific investigation's needs, researchers in need of quantitative results may be advised to use the electron microprobe. In some instances, however, the area of interest is simply too small and must be analyzed by TEM (where EDS is the only option) or high resolution SEM (where the low beam currents used preclude WDS, making EDS the only option).

#### *EDS Artifacts*

System peak, escape peaks and sum peaks, are all phenomena that an EDS user must be aware of. Modern analytical software used in processing energy dispersive x-ray spectra can generally take them into account -- but such software is not perfect. Also, many users will look at the raw spectra, where the software may or may not have labeled the artifacts.

*Peak overlaps* - the spectral resolution of EDS is not as great as WDS. Resolution is usually defined as the FWHM (full width at half maximum) of pure Mn Ka: ~ 150 eV. Therefore, the separation of some peaks can be poor. Examples include the case where small amounts of Fe are being investigated in the presence of large amounts of Mn (Mn Kb is very close to Fe Ka), and the case where Cu, Zn and Na are present together: the L lines of Cu and Zn are close to the K lines of Na.

This figure shows the problem of attempting to analyze a Ti-V alloy with a trace amount of Cr. Because of the ubiquitous k-beta overlaps in this region of the periodic table, we have a cascade overlaps situation of a major concentration of Ti interfering with minor amount of V, which in turn significantly interferes with a trace concentration of Cr. This is a situation that definitely requires special handling to obtain quantitative results, the overlap on the trace concentration is approximately 1000%. However, much more simple and commonly encountered cases of minor spectral overlap often occur and the analyst is required to be aware of these difficulties.

One classic case was a paper published where Al was reported in the brains of patients with Alzheimer's disease, but was eventually shown to be caused by the mis-identification of a minor spectral line from osmium (in osmium tetroxide used to prepare the sample) as the Al ka line.

### *Wavelength Dispersive Spectrometry (WDS)*

WDS was the original electron microprobe spectroscopy technique developed to measure precisely x-ray intensities and hence accurately determine chemical compositions of microvolumes (a few cubic microns) of "thick" specimens, and the instrument used is the electron microprobe. In the 1960-70s there were roughly half a dozen companies commercially producing them; today, there are only two (JEOL and CAMECA). A full-package An electron microprobe today costs \$500-\$750,000.

The key feature of the electron microprobe is a crystal-focusing spectrometer, of which there are usually 3-5, although one manufacturer in 1970-80 produced a 9 spectrometer instrument that are still much in use.

### **WDS Schematic**

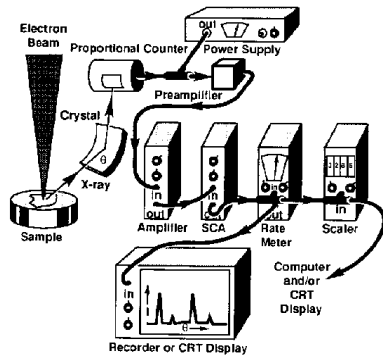


**Figure 5.1.** Schematic representation of a wavelength-dispersive spectrometer and associated electronics.

from J. I. Goldstein, D. E. Newbury, P. Echlin, D. C. Joy, C. Fiori, E. Lifshin, "Scanning Electron Microscopy and X-Ray Microanalysis", 2nd Ed., Plenum, New York, 1992

### **WDS focal circle figure**

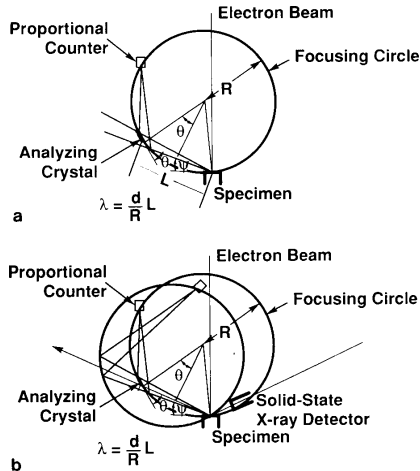


**Figure 5.3.** (a) Fully focusing wavelength-dispersive spectrometer.  $R$  is the radius of the focusing circle,  $\psi$  is the take-off angle, and  $\theta$  is the diffraction angle. (b) Movement of the focusing circle to change the diffraction angle. Note position of EDS detector at the same take-off angle.

from J. I. Goldstein, D. E. Newbury, P. Echlin, D. C. Joy, C. Fiori, E. Lifshin, "Scanning Electron Microscopy and X-Ray Microanalysis", 2nd Ed., Plenum, New York, 1992

X-rays (as well as many other excited particles and radiations) are produced in the "interaction volume" immediately below the impact zone of the finely focused electron beam. A very small fraction of all x-rays will be emitted at the proper "take-off" angle to enter the WDS spectrometer acceptance angle (a much smaller fraction compared to an EDS detector mounted a few cms from the sample). Remember each element's characteristic x-ray has a distinct wavelength, and by adjusting the tilt of the crystal in the spectrometer, at a specific angle it will diffract the wavelength of specific element's x-rays, according to Bragg's Law:

$$n\lambda = 2d \sin \theta$$

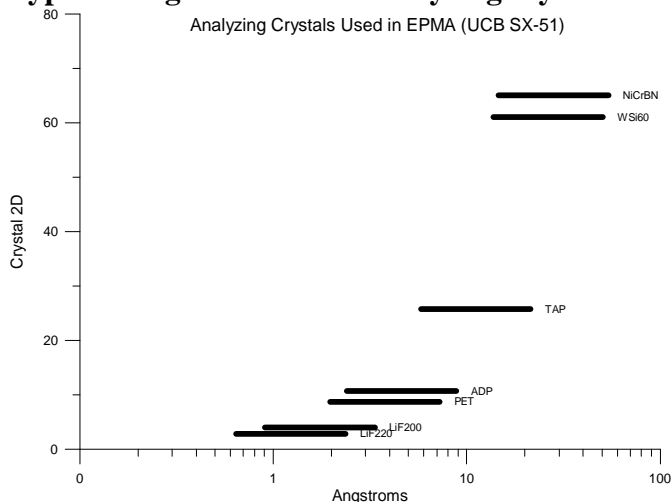
Those diffracted x-rays are then directed into a gas-filled proportional counting tube, which has a thin wire (usually tungsten) running down its middle, at 1-2 kV potential. The x-rays are absorbed by gas molecules (e.g., P10: 90% Ar, 10% CH<sub>4</sub>) in the tube, with photoelectrons ejected; these produce a secondary cascade of interactions, yielding an amplification of the signal (approx.  $10^6$ ) so that it can be further amplified by the counting electronics.

The voltage pulse produced by the incoming x-ray is accompanied by a large number (in fact an infinite number with an amplitude of zero volts) of randomly generated noise pulses of a much lower voltage. These noise pulses must be rejected before the signal is pulse counted and this is the role of pulse height analysis (PHA). Simply, special electronic circuits are adjusted so that only pulses with a certain range of energies or pulse heights (greater than the "baseline" and less than the "window") are allowed to enter the scaler electronics for counting.

Different diffracting crystals, with 2d (lattice spacings) varying from 2.5 to 200 Å, are used to be able to diffract various ranges of wavelengths that may correspond to the primary emission lines of various elements. In recent years, the development of "layered synthetic crystals" of large 2d has led to the ability to analyze the lower Z elements (Be, B, C, N, O), although inherent limitations in the physics of the process (e.g., large loss of signal by absorption in the sample) limit the applications.

Here is a graph which illustrates the typical range of applicability for the various crystals found in many electron microprobes:

**Typical ranges for various analyzing crystals:**



*Comparison of EDS to WDS*

EDS can also be used to get quantitative chemical information in many situations, and the following is a comparison made at equal and optimized conditions for each method:

**Comparison of EDS to WDS, Equal Beam Current (from Goldstein, et. al. 1988), pure Si and Fe, 10<sup>-11</sup> A (0.01 nA), 25 keV**

	60 sec	P (cps/10 <sup>-8</sup> A)	P/B	C <sub>DL</sub> (ppm)
Si Kα	EDS	5400	97	580
	WDS	40	1513	1,710
Fe Kα	EDS	3000	57	1,000
	WDS	12	614	4,900

**Comparison of EDS to WDS, Optimized Conditions (from Goldstein, et. al. 1988), 15 keV, 180 seconds counting time:**

**EDS : 2 x 10<sup>-9</sup> A (2 nA) to give 2K cps spectrum to avoid sum peaks**

**WDS : 3 x 10<sup>-8</sup> A (30 nA) to give 13K cps on Si spectrometer (> 1 % dt)**

		Peak cps	P/B	C <sub>DL</sub> (ppm)
EDS	Na Kα	32.2	2.8	1,950
	Mg Kα	111.6	6.4	1,020

	Al K $\alpha$	103.9	5.7	690
	Si K $\alpha$	623.5	22.8	720
	Ca K $\alpha$	169.5	8.5	850

WDS	Na K $\alpha$	549	83	210
	Mg K $\alpha$	2183	135	120
	Al K $\alpha$	2063	128	80
	Si K $\alpha$	13390	362	90
	Ca K $\alpha$	2415	295	90

Here are some cases where WDS is the preferred technique, if available:

- where greater precision is required (WDS can handle significantly higher count rates)
- where the peaks are too close in EDS to be resolved (typically EDS resolution is  $\sim 150$  eV, versus WDS which is  $\sim 5$  eV)
- where trace element levels are desired, WDS has a higher P/B, yielding lower minimum detection limits.

WDS does not usually suffer from pulse pileup (too many counts coming in, i.e. from major elements) that occurs in EDS, and which must be compensated for mathematically.

WDS has different spectral artifacts, compared with EDS: for WDS, one unique problem that may occur is if a higher order reflection ( $n > 1$ ) of a line falls near the line of interest and this will be discussed in the section on spectral interference below.

### *Background correction*

The background correction in EPMA is required because of the production of continuum radiation from inelastic collisions by the incident electrons in the specimen. This radiation is the primary source of background in EPMA and is the limiting factor for minimum detection limits for the technique.

### **Continuum production figure**

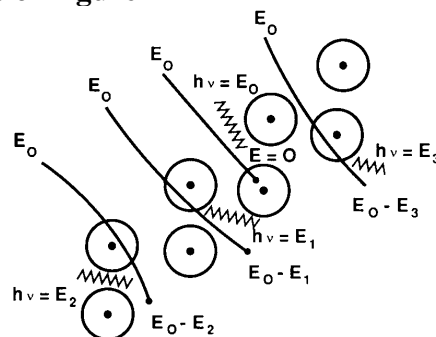
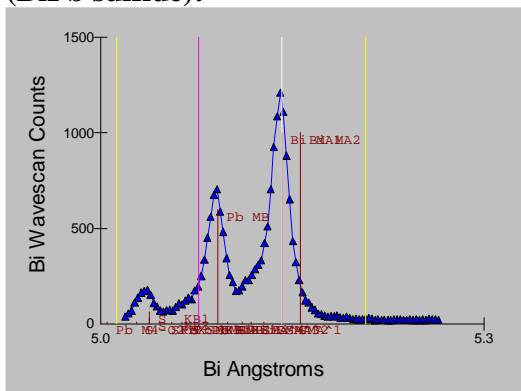


**Figure 3.31.** Schematic illustration of the origin of the x-ray continuum, resulting from deceleration of the beam electrons in the Coulombic field of the atoms.

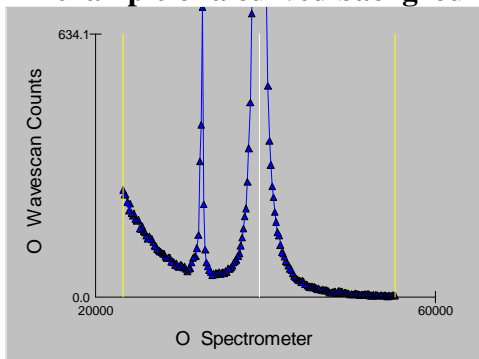
Two methods are used for background correction, the most common method is the so called “off-peak” method which measures the background due to the continuum on either side of the characteristic peak. There is also an alternative method for the correction of background based on the fact that the intensity of the continuum ( $I_C$ ) is a function of the mean atomic number ( $\bar{Z}$ ) of the sample.

Assuming that the off peak offsets are appropriate and no other peaks interfere with the measurement, the intensities may be linearly interpolated and subtracted from the peak intensity. In certain cases it may be desired to utilize a measurement only on one side of the peak or to average the off-peak measurements, however since the continuum is usually sloped and the background offsets may not be symmetrical about the characteristic peak, care must be taken with such procedures.

**An example of the necessity of carefully selecting off-peak background positions (BiPb sulfide):**



**An example of a curved background (MgO):**



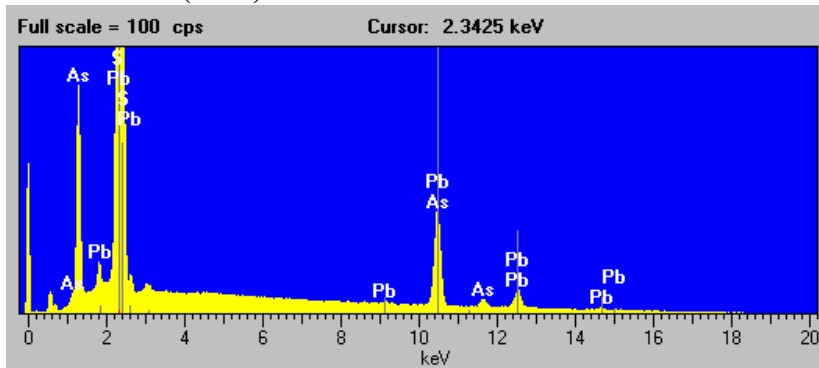
*Peak interferences*

As mentioned earlier, one unique WDS spectral artifact are the higher order lines implied by Bragg’s law in which a higher energy line can diffract at the same wavelength. However, WDS can in many cases eliminate that higher order line, by fine tuning the proportional counter electronics, applying "pulse height analysis" to energy filter out the unwanted x-rays since the higher order lines, although of similar wavelength are much higher in energy. In the case of some primary (n=1) overlapping lines, even for WDS,

correction for spectral interference may be required, e.g. for V K $\alpha$  in the presence of abundant Ti (K $\beta$  interference) or for B K $\alpha$  in the presence of abundant Mo (M-line interference).

Here is an EDS spectra, of an unknown ore mineral, again acquired with a pulse processing time configured for maximum energy resolution.

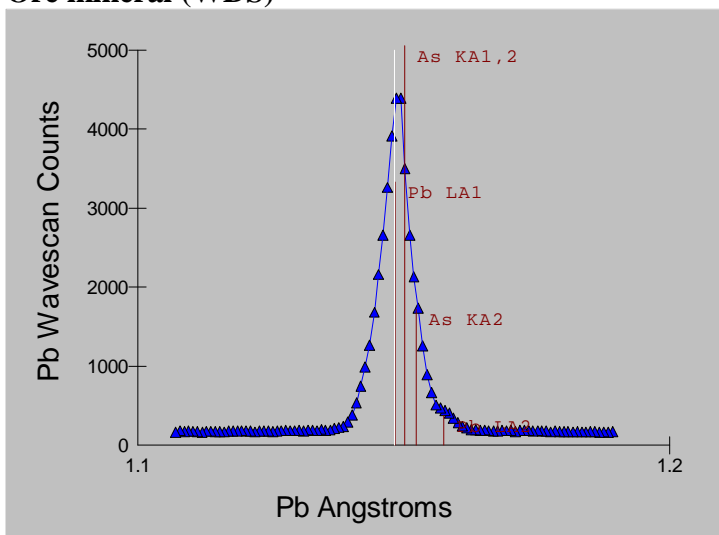
### Ore mineral (EDS)



Not a very pretty picture, since we cannot separate the Pb L $\alpha$  and As K $\alpha$  peaks or the Pb M $\alpha$  and S K $\alpha$  peaks. From a qualitative viewpoint we can only state that it is at least evident that that As is present from the appearance of the As L $\alpha$  line and Pb likely present from the appearance of the secondary L lines, although S is interfered strongly by the Pb M $\alpha$  line and can only be inferred by the mineralogy.

Here now we have the same ore mineral sample, and it's spectra acquired in the vicinity of the Pb L $\alpha$  and As K $\alpha$  lines, using a WD spectrometer equipped with an LiF analyzing crystal with an approximate energy equivalent resolution of 10 eV.

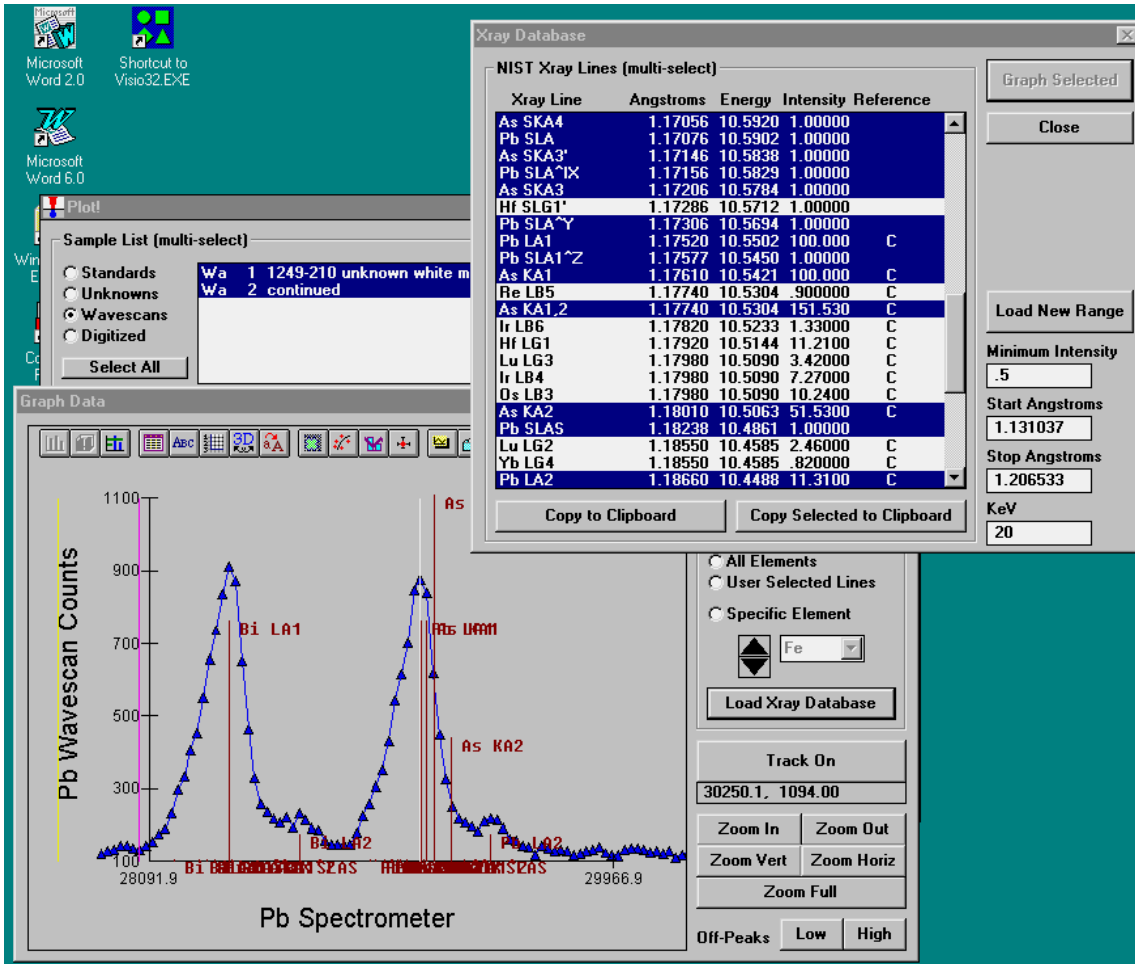
### Ore mineral (WDS)



As can be seen in this figure, even with the kind of resolution available with WDS, we still have large overlaps that will create confusion with qualitative analysis and much difficulty when we attempt quantitative analysis.

*Qualitative Analysis*

Qualitative analysis is the identification of the elements present in the specimen. No attempt is generally made to estimate concentrations other than major, minor, trace although even this can be difficult in many cases due to large differences in absorption between the various x-ray lines.



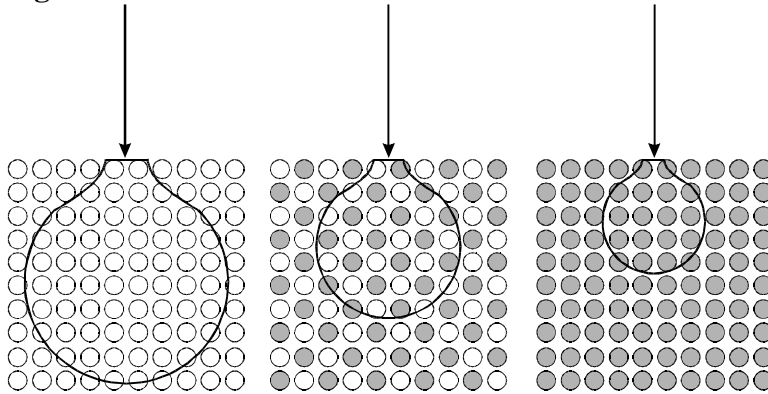
### Quantitative analyses (Theoretical Basis)

The first attempt to quantify the production of x-rays in materials was made in 1951 by Raymond Castaing, as his Ph.D. thesis at the University of Paris. Castaing proposed first, utilizing a standard along with the unknown specimen, for purpose of determining the ratio of x-ray intensities in order to eliminate calibrations pertaining to spectrometer efficiency, and second, that the ratio of those intensities could be scaled to elemental mass fraction within the specimen, seen here:

$$\frac{c_i^u}{c_i^s} = \frac{I_i^u}{I_i^s} \quad (1)$$

Now let's consider, for a moment, atomic fraction averaging as a basis for modeling electron-solid interactions, which at first might seem more reasonable, although, it is evident to everyone that has worked in this area, that simple atomic fraction utterly fails to accurately describe the proportion of x-ray production contributed by the various atoms in a compound. Why is this?

**Figure 4**



In this figure, adapted from Reed (1993), we schematically depict the penetration effect of the incident electron beam for a binary compound, where we have a low Z element here, a high Z element here, and in the center, a compound consisting of equal numbers of low Z and high Z atoms. It is evident, by simply comparing the number of colored circles within the interaction volumes, that the compound will contain almost as many atoms of the high Z element, as it's pure element, but only a small fraction of the low Z element, compared to it's pure element.

Because of this disproportionality, Reed postulated that the electron beam penetrates an interaction volume of constant mass for compounds of different composition. In fact, this is only approximately true because the proportion of atomic weight (i.e., mass) to atomic number (electron interactions) or  $A/Z$ , is approximately a constant, because from isotope studies, it is known that the neutron has no effect on electron solid interactions at these energies.

In any case, a significant complication arises because we are dealing with a "thick" specimen (more than a few microns thick): absorption of X-rays, particularly long wavelength, lower energy ones, can be an important factor in reducing the number of certain X-rays counted, compared to those generated in the sample.

In addition to this absorption correction (A), corrections need also be made for fluorescence (F: the generated X-rays may also produce additional X-rays of other lines in the sample) and for 'atomic number effects'(Z). These three corrections are the matrix correction, ZAF, based upon various physical models developed to describe these effects, seen here:

$$k_i = c_i Z_i A_i F_i \quad (2)$$

Traditionally, analysts have utilized mass fraction for proportioning these inter-element effects, although as already noted above, mass is not directly involved.

In the past, analysts have attempted to improve the accuracy of their analyses by selecting standards that are similar in composition to the unknowns, so that there are no large extrapolations. However, due to improvements in the algorithms used for calculation of matrix effects, the use of poorly characterized standards now produce the largest errors. To avoid that, we often utilize, whenever possible, pure element or simple oxide standards (MgO, Al<sub>2</sub>O<sub>3</sub>, SiO<sub>2</sub>, TiO<sub>2</sub>, etc.) that have a known stoichiometric composition.

Standards of this type may not always be possible to obtain (e.g., Na<sub>2</sub>O, K<sub>2</sub>O), and in those cases, and for the purposes of using secondary standards as a check on the quality of the analyses, we can utilize standards whose compositions have been determined by classical wet-chemistry or other gravimetric techniques, and that similar in composition to the unknown.

#### *Absorption Correction*

Absorption is often the largest correction made to the x-ray intensities in quantitative microanalysis and therefore the accuracy with which we calculate the correction most directly influences the accuracy of the quantitative results that we may obtain. The absorption is defined as the absorption of an x-ray by the atoms present in the sample

Traditionally absorption is considered a one of the terms in the ZAF correction, but within the last few decades much work has been done to describe the absorption correction as a function of the depth distribution of the generated x-rays within the sample. Therefore both factors for x-ray absorption and electron scattering (electron and energy loss) are considered at the same time. This is called the  $\phi\rho z$  curve method.

In either case, the most important parameters for the correction are

1. incident electron energy
2. x-ray takeoff angle

### 3. mass absorption coefficients

The incident energy of the electron beam can be determined by careful measurements of the continuum in the region where the overvoltage approaches zero also known as the Duane-Hunt limit. Use of this technique can determine the true accelerating voltage to within 50 volts or so.

The x-ray take-off angle can not be directly measured except by comparison of k-ratios for opposite pairs of spectrometers.

Mass absorption values which describe the photo-absorption of x-rays in the various elements have been the subject of intense experimental effort, especially for those x-ray energies equal to the emission line energies.

	Heinrich (CITZAF)	Henke (1982)
Mg K $\alpha$ in Si	802	859
<b>Mg K<math>\alpha</math> in Fe</b>	<b>6121</b>	<b>5250</b>
Si K $\alpha$ in Mg	2825	2902
Si K $\alpha$ in Fe	2502	2305

As one can see there is about 20% difference in the mass absorption coefficients for Mg K $\alpha$  in Fe although the others are reasonably close. This difference will have a significant effect on the quantitative analysis (about 1 % or so) in this case.

#### *Atomic Number Correction*

The atomic number correction is used to describe electron scattering in specimens of various composition. The two primary mechanisms creating the atomic number effect are changes in trajectory due to high angle scattering that cause little or no reduction in the energy of the electron (elastic scattering) and can result in a significant loss of electrons backscattered out of the sample and hence no longer involved in the production of characteristic x-rays and reduction in energy of the incident electrons involved in various elastic processes such as continuum and characteristic x-ray production as well as phonon, auger, and secondary electron production.

This correction may be calculated separately or combined in the  $\phi\rho z$  curve method along with the absorption correction.

#### *Fluorescence Correction*

The fluorescence correction is required due to the fact that not only can electrons cause x-ray fluorescence but x-rays generated by the electron beam (primary) can also cause additional x-ray fluorescence (secondary) in other elements that may also be present.

The complete form of the correction (along with an analogous correction for spectral interference) is shown here:

$$C_A^u = \frac{C_A^s}{[ZAF]_{1A}^s} [ZAF]_{1A}^u \frac{I^u(I_A) - \frac{[ZAF]_{1A}^{\bar{s}}}{C_B^{\bar{s}}} \frac{C_B^u}{[ZAF]_{1A}^u} I_{B}^{\bar{s}}(I_A)}{I_A^s(I_A)}$$

Where the following notation has been adopted :

- $C_i^j$  is the concentration of element i in matrix j
- $[ZAF]_{\lambda_i}^j$  is the ZAF (atomic #, absorption and fluorescence) correction term for matrix j (Z and A are for wavelength  $\lambda_i$  and F is for the characteristic line at  $\lambda_i$  for element i)
- $I_i^j(\lambda_i)$  is the measured x-ray intensity excited by element i in matrix j at wavelength  $\lambda_i$
- $\bar{s}$  refers to an interference standard which contains a known quantity of the interfering element B, but none of the interfered element A

### Precision

Precision is often defined as the “reproducibility” of the measurement. In other words, “what is the probability that if the measurement is repeated, we will obtain the same result”?

Because the microprobe is based on x-ray counting statistics, the “significance” of the measurement is intimately related to the number of counts that we obtain. Consider that if we count for a short enough time (or at a low enough count rate), so that we obtain only a single count, the chances are roughly 50/50 that the next measurement (under the same conditions) will again produce a single count. About half the time, we will obtain no counts. So our precision error is 100%.

By counting longer (and/or at higher count rates using more voltage and beam current) we will increase the total number of counts obtained and hence decrease the counting error.

Because at high count rates, x-ray counting statistics can be described by essentially Gaussian statistics (low count rates are more accurately described by Poisson statistics due to the fact that we cannot measure less than zero counts), we can easily predict the precision of a measurement based simply on the total number of measured counts as shown in the following table:

### Precision in EPMA is related to count rate (at low to moderate cps)

Total number of counts	Approximate precision (assuming normal gaussian statistics)	Approximate time to acquire (assuming 1K counts/sec)
------------------------	---	--

100	10%	0.1 sec
1,000	3.1%	1 sec
10,000	1%	10 sec
100,000	0.31%	100 sec
1,000,000	0.1%	1000 sec

Total number of counts	Approximate number of significant digits (assuming 99% confidence)
100	<1
1,000	2
10,000	<3
100,000	3
1,000,000	<4

### Accuracy

Accuracy is best thought of as the answer to the question “how close is the measurement to the true answer?”. In EPMA, we are helped by the fact that many difficult to determine parameters, such as spectrometer and detector efficiency, are eliminated by the use of standards measured under the same conditions as our unknown. However, we are limited in accuracy by the performance of the various matrix corrections that are employed, when the standard differs from the unknown, in the emission of characteristic x-rays.

Of course, since we can never actually know the “true” answer, we must use indirect methods to calculate accuracy. One method is to compare a measurement to a measurement of a standard, ideally similar to our unknown. By comparing our ability to measure well characterized standards among themselves, we can gain some knowledge of the accuracy of our measurements. The following table shows some typical accuracies on the microprobe.

### Typical Accuracies for Elements of Geologic Interest

#### Fe Analyses

“Primary” standard	Fe <sub>3</sub> O <sub>4</sub> (magnetite)	magnetite	magnetite	Fe
“Secondary” standard	FeCr <sub>2</sub> O <sub>4</sub> (chromite)	Fe <sub>2</sub> SiO <sub>4</sub> (fayalite)	chromite	FeS <sub>2</sub> (pyrite)
Measured	10.114	54.655	20.788	46.796
“Published”	10.136	54.809	20.692	46.550
Percent Variance	-0.22	-0.28	0.46	0.53

#### Si Analyses

“Primary” standard	SiO <sub>2</sub> (quartz)	SiO <sub>2</sub>	SiO <sub>2</sub>	
“Secondary” standard	fayalite	Na <sub>3</sub> (Na,K)[Al <sub>4</sub> Si <sub>4</sub> O <sub>16</sub> ] (nepheline)	(K,Na)[AlSi <sub>3</sub> O <sub>8</sub> ] (orthoclase)	
Measured	13.690	20.242	29.739	
“Published”	13.785	20.329	30.286	
Percent Variance	-0.69	-0.43	-1.81	

### Mg Analyses

“Primary” standard	MgO	MgO		
“Secondary” standard	chromite	diopside		
Measured	9.229	11.311		
“Published”	9.166	11.192		
Percent Variance	0.69	1.06		

### Al Analyses

“Secondary” standard	nepheline	orthoclase	chromite	
“Primary” standard	Al <sub>2</sub> O <sub>3</sub>	Al <sub>2</sub> O <sub>3</sub>	Al <sub>2</sub> O <sub>3</sub>	
Measured	17.607	8.379	5.181	
“Published”	17.868	8.849	5.250	
Percent Variance	-1.46	-5.31	-1.32	

In practice, there are two ways to proceed. The first method is that by using standards as close as possible in composition to the unknown, and by assuming that the standard compositions are accurately known, because the matrix correction for an unknown that is identical in composition to the standard is exactly 1.000, we can eliminate errors due to the matrix correction itself. However, it is not always possible to find standards with similar compositions to our unknowns.

The problem with this assumption is that the accuracy of the standard composition itself is not always known. While it is easy to believe that pure Si is 99.999% Si (if we can detect no trace elements) and even pure SiO<sub>2</sub>, may be said to be 99.999% SiO<sub>2</sub>, if similar in purity, it is quite a different thing to know the composition of a more complex compound that is not restricted by purity or stoichiometry (which is normally the case for a standard close in composition to our unknown).

For example, an olivine standard requires that Mg, Fe and Si be known (assuming that oxygen may be calculated by stoichiometry). But because there is a solid solution from pure Fe<sub>2</sub>SiO<sub>4</sub> to Mg<sub>2</sub>SiO<sub>4</sub>, we cannot by simple stoichiometry “know” the true composition of the olivine standard. In an attempt to determine the “true” composition of Fe and Mg, it is required that these be measured independently of the microprobe. One common method is so called “classical” wet chemical methods based on gravimetric (weighing) measurements.

This means that our wet chemical precision is related to the reproducibility of our weighing, mixing and diluting and the accuracy is related to the accuracy of the scale. In fact wet chemical methods have their own systematic errors that affect the accuracy of the determination of the standard composition. For example, when Al is precipitated out of solution in preparation for weighing, significant Fe may also be precipitated. It is unlikely that these systematic errors in wet chemistry would cancel any systematic errors inherent in EPMA methods.

The other way to proceed with our measurements, is to utilize pure elements or simple oxides and assume that due to purity and constraints of stoichiometry (for simple oxides), that the compositions are accurately known. We then rely solely on the accuracy of the matrix corrections themselves. The accuracy of the matrix correction may be determined by careful comparison of well characterized “secondary” standards. Once again, we need to judge the accuracy of these secondary standards, but it is possible, for example, that by measuring Si Ka in a pure Mg<sub>2</sub>SiO<sub>4</sub> against a pure SiO<sub>2</sub> standard, we might be able to assign a confidence in how well we can matrix correction the effect Mg on Si Ka. Since both materials can be obtained pure and may be considered stoichiometric, any error in that measurement might be considered a measurement of the accuracy of the matrix correction (for that particular case at least).

### *Trace elements*

Trace elements are those measurements where due to numerous factors, the signal level of our measurement is similar to the measurement of the background itself.

The background in the microprobe is almost entirely due to the production of continuum x-rays from the deceleration of the primary beam electrons in the sample. This presence of this continuum, is the limiting factor for trace elements detection in the microprobe.

To circumvent this limitation of the electron beam, some effort has been made to develop focused x-ray beams which produce much lower x-ray backgrounds. Due to the difficulty in focusing x-ray beams this still remains expensive is usually found only in large synchrotron beam lines.

What signifies the detection of an element? Assuming again Gaussian statistics, it is usually stated that any measurement that exceeds 3 times the standard deviation of the background has a 99% confidence of being “real” (that is, truly present).

Since the standard deviation may be described as the square root of the background counts, the calculation may be performed utilizing the formula given here, adapted from Love and Scott (1974).

$$CDL = (ZAF) \frac{3}{I_S} \sqrt{\frac{I_B}{t}} \cdot 100$$

Where :

ZAF	is the ZAF correction factor for the sample matrix
I <sub>S</sub>	is the count rate on the analytical (pure element) standard
I <sub>B</sub>	is the background count rate on the unknown sample
t	is the counting time on the unknown sample

An analogous calculation which describes the analytical sensitivity of the measurement can also be calculated from similar information. The analytical sensitivity is the precision of a

measurement and allows one to assign a confidence that two measurements that differ, are in fact different.

This expression, also from Love and Scott, is usually multiplied by a factor of 100 to give a percent analytical error of the net count rate.

$$\epsilon_{P-B} = \frac{\sqrt{\frac{N_P}{t_P^2} + \frac{N_B}{t_B^2}}}{\left(\frac{N_P}{t_P} - \frac{N_B}{t_B}\right)}$$

Where :

- $N_P$  is the total peak counts
- $N_B$  is the total background counts
- $t_P$  is the peak count time
- $t_B$  is the background count time

Calculations based on the actual measured standard deviation of the measurement is useful for several reasons. First it allows us to determine if the variation in the measurements is due to actual variation in the sample or simply to the statistics.

Secondly, once the level of homogeneity for the sample is known, we can determine the worst case analytical sensitivity since the measured standard deviation also includes variability from instrument drift, x-ray focusing, surface and coating variability.

The following expressions are based on equations adapted from "Scanning Electron Microscopy and X-Ray Microanalysis" by Goldstein, et. al. (Plenum Press, 1992 ed., 1981) p. 432 - 436.

1. The range of homogeneity in plus or minus weight percent.

$$W_{1-\alpha} = \pm C \frac{t_{n-1}^{1-\alpha}}{n^{1/2}} \frac{S_C}{\bar{N}}$$

2. The level of homogeneity in plus or minus percent of the concentration.

$$\pm \frac{W_{1-\alpha}}{C} = \pm \frac{(t_{n-1}^{1-\alpha}) S_C (100)}{n^{1/2} \bar{N}}$$

3. The trace element detection limit in weight percent.

$$C_{DL} = \frac{C_S}{\bar{N}_S - \bar{N}_{SB}} \frac{2^{1/2} (t_{n-1}^{1-\alpha}) S_C}{n^{1/2}}$$

4. The analytical sensitivity in weight percent.

$$\Delta C = C - C' \geq \frac{2^{1/2} C (t_{n-1}^{1-\alpha}) S_C}{n^{1/2} (\bar{N} - \bar{N}_B)}$$

- Where :
- $C'$  is the concentration to be compared with
  - $C$  is the actual concentration in weight percent of the sample
  - $C_S$  is the actual concentration in weight percent of the standard
  - $t_{n-1}^{1-\alpha}$  is the Student t for a  $1-\alpha$  confidence and  $n-1$  degrees of freedom
  - $n$  is the number of data points acquired
  - $S_C$  is the standard deviation of the measured values
  - $\bar{N}$  is the average number of counts on the unknown
  - $\bar{N}_B$  is the continuum background counts on the unknown
  - $\bar{N}_S$  is the average number of counts on the standard
  - $\bar{N}_{SB}$  is the continuum background counts on the standard

#### Optimal Detection Limits on the Electron Microprobe

element (x-ray line)	matrix	voltage (KeV)	current (nA)	$C_{DL}$ (ppm)	count time (sec)
----------------------	--------	---------------	--------------	----------------	------------------

<b>Al (Ka)</b>	quartz	20	100	20	640
<b>Fe (Ka)</b>	quartz	20	100	30	640

<b>Ge (Ka)</b>	Fe-Ni meteorite	35	200	20	1800
<b>C (Ka)</b>	Fe	10	50	300	1800

<b>Ca (Ka)</b>	olivine	15	200	13	2400
<b>Al (Ka)</b>	olivine	15	200	18	2400
<b>Ti (Ka)</b>	olivine	15	200	25	2400
<b>Cr (Ka)</b>	olivine	15	200	13	2400
<b>Mn (Ka)</b>	olivine	15	200	14	2400
<b>Ni (Ka)</b>	olivine	15	200	14	2400
<b>P (Ka)</b>	olivine	15	200	14	2400
<b>Na (Ka)</b>	olivine	15	200	13	2400

### *Volatile element Correction*

Some element intensities may vary over time with exposure to the electron beam. This may be observed as either an increase or decrease in intensity over time. Since this effect is typically observed as a loss in intensity it is often referred to as a volatile element loss.

There are several proposed mechanisms for these effects including temperature and sub-surface charging. To see the effect that temperature could have on the specimen, here are some calculations for beam induced heating in various samples:

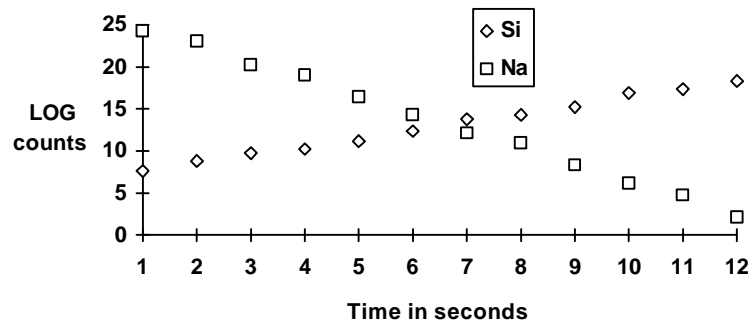
$$\Delta T = 4.8 \cdot \left( \frac{E_0 i}{kd} \right)$$

Where :  
 $E_0$  = electron beam in KeV  
 $i$  = beam current in uA  
 $k$  = thermal conductivity in watts cm-1 K-1  
 $d$  = beam diameter in um (microns)

Material	$k$	DT °K (15 keV, 0.02 uA, 2 um)	DT °K (20 keV, 0.05 uA, 2 um)
obsidian glass	0.014	51	171
zircon	0.042	17	57
quartz	0.10	7.2	24
calcite	0.05	14	48
mica	0.006	120	400
iron metal	0.80	0.9	3
epoxy	0.002	360	1200

This is often the case for volatile elements such as sodium or potassium, but the extrapolation correction can also be applied to any degradation (or enhancement) of the x-ray intensities over time due to other causes such as sample damage, carbon contamination, etc. This correction is especially useful for samples which are too small to utilize a defocused beam and allows the user to run higher sample currents to improve the analytical sensitivity.

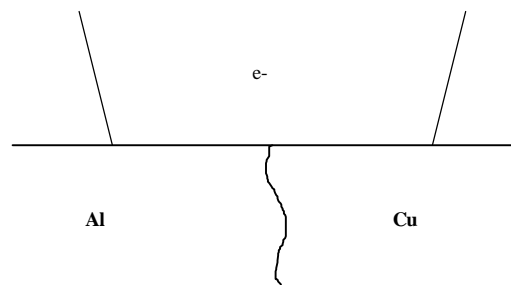
For instance, when sodium loss is observed in an alkali glass sample, a corresponding gain in silicon and aluminum x-rays may be noted. The extrapolation correction used in Probe for Windows can be applied to some or all elements in a sample, regardless of whether the x-ray intensities are decreased or increased during the acquisition (**as long as the elements to be corrected are acquired as the first element on each spectrometer, i.e., order number = 1**). The correction assumes that the change in counts is linear versus time when the natural LOG of the x-ray counts are plotted (Nielsen and Haraldur, 1981) as shown here :



Depending on the sample, this may or may not be a valid assumption. Under certain conditions, with very volatile hydrous alkali glasses, the change in count rate may actually decrease more quickly than a simple log decay. In this case, it may be necessary to defocus the beam slightly before acquisition.

*Sample Homogeneity on the Scale of the Beam Size*

Consider the extreme situation depicted below. An interface of Al and Cu metal where the electron beam excites x-rays from both sides of the interface.



In this situation, x-rays of both metals will be produced. However, note that because the Cu x-rays are generated mostly in a pure Cu matrix and the Al x-rays are mostly generated in an pure Al matrix, the actual matrix correction that needs to be applied to the measured x-rays will be different than simply the matrix correction for a homogenous alloy sample consisting of both Al and Cu.

Now, as you may know, the matrix correction for the x-ray of an element in the pure element is considered to be 1.0. Hence for the majority of the x-rays produced in this sample, the matrix correction that needs to be applied to each x-ray is very close to 1.0 since, as stated above, most of the Cu x-rays are generated in a pure Cu matrix and most of the Al x-rays are generated in a pure Al matrix. However, when the microprobe measures the x-ray intensities at this boundary and receives both Al and Cu x-rays, it knows nothing of the actual geometry, and can only assume that all the x-rays measured are to be matrix corrected using a composition that is determined by iteratively correcting the measured x-ray intensities. This is the nature of the ZAF or phi-rho-z matrix correction. Of course, one could apply a geometric model to the matrix correction to

correct for the interface effect, but this would require precise knowledge of the interface shape and orientation which is usually not available.

Since determining the geometry of a buried interface is difficult if not impossible, the software can only assume a matrix correction based on a composition consisting of both Cu *and* Al, since both x-rays were detected. The matrix correction for Al x-rays in a homogenous Cu-Al alloy is of course quite different than that of pure Al, which is really the situation that created the Al x-rays in our example and the same is true for the Cu x-rays as well. The effect of assuming a homogenous matrix, when in fact the sample is very inhomogenous, is to apply the wrong matrix correction to the x-rays detected from the sample.

The following is a calculation for the correction of Cu  $k\alpha$  and Al  $k\alpha$  x-rays in a 50:50 homogenous alloy at 15kV and a 52.5 degrees takeoff angle :

50:50 Cu-Al alloy	Cu	Al
Elemental k-ratio	0.45732	0.34037
ZAF correction	1.0933	1.4690

As you can see, the correction for both x-rays, but especially Al  $k\alpha$  (47% ZAF correction), is significantly higher than the correction for each x-ray in the pure element (1.0). This will result in a very high total as the beam straddles the interface between the two phases, since both x-rays will be over corrected by homogenous alloy composition matrix correction. This example is extreme, but the situation applies to any inhomogenous sample in which the matrix correction for the different phases present are not equal. This is because the matrix correction itself is non-linear and cannot be applied to the normalized x-ray intensities generated from the different phases.

It is best to remember the words of the late Chuck Fiori, who said : "if the feature is smaller than the size of the beam, then all bets are off".

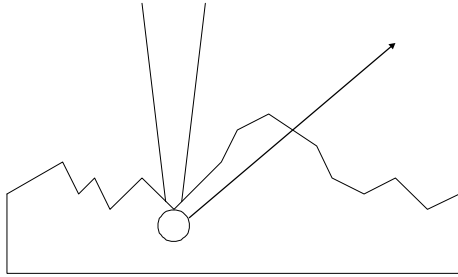
It is also important to remember that when the sample inhomogeneity is much smaller than the scale of the beam (for example particle phases less than 0.05 microns), that this effect becomes insignificant due to the fact that the many phases involved in the production and absorption of the x-rays tend to average out the contribution from a single phase. Of course this also means that it is possible to only determine the *average* composition of very fine grained materials. But at least we don't have to worry about inhomogeneity on the atomic scale!

#### *Sample preparation*

Poor sample preparation- rough surfaces can preferentially bias the analysis against low energy x-ray as seen in this figure,

#### **Rough surface figure**

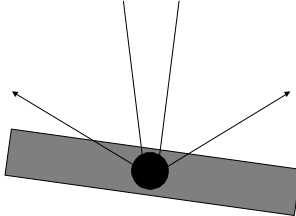
Rough surface problems:



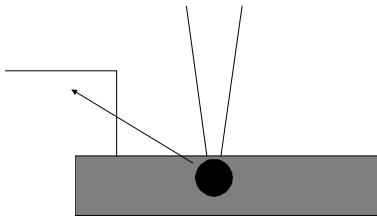
Conductive coatings (if any) must be carefully applied to clean surfaces and is required to be of the same composition and thickness for both the standard and the unknown sample. In many cases, (light element analysis) this may require that the standards and unknowns be coated at the same time.

### Problems with sample geometry

Tilted sample problems:



Line of sight problems:



Incorrect sample geometry - X-rays emerge from a sample and travel line - of -sight trajectories. Thus, if the sample is tilted incorrectly, something may actually block the path between detector and sample.

This will manifest itself either as an inordinately low number of X-rays (expressed as counts sec-1) or you may notice an absence of low energy X-rays (either due to blocking or re-absorption) in the spectrum being collected. This is not normally a concern on the microprobe where specimens are polished flat, although it can occur when the analyzed area is near the edge of the mounted sample as seen in the above figure.

### Carbon coat thickness variation

Variations in the thickness of the carbon (or other conductor) coat, can result in a difference in intensity emitted from the specimen surface. This may result from two different mechanisms.

In the first, soft x-ray emitted from the sample are absorbed by the coating, hence if the absorption is significant enough, then differences in the thickness of the coating between the standard and the unknown will produce a difference in the intensity of the x-ray detected from the sample and standards. Due to the non-linear and complex nature of the absorption (absorption edges) it is not possible to make a general statement regarding the magnitude of the effect. The following table gives several examples for absorption of several commonly measured soft x-rays in carbon coats of three different thicknesses:

**Percent x-ray transmission (assume density of carbon is 2.7 gm/cm<sup>3</sup>):**

	10 nm (carbon)	20 nm (carbon)	40 nm (carbon)
Ti K $\alpha$ (19.76)	0.99994	0.99989	0.99978
Si K $\alpha$ (356.8)	0.99903	0.99807	0.99615
Al K $\alpha$ (557.2)	0.99849	0.99699	0.99400
Mg K $\alpha$ (904.8)	0.99756	0.99512	0.99027
Na K $\alpha$ (1534)	0.99586	0.99175	0.98356
F K $\alpha$ (6366)	0.98295	0.96620	0.93355
O K $\alpha$ (12,380)	0.96712	0.93533	0.87484
N K $\alpha$ (25,490)	0.93349	0.87140	0.75935

Another way in which the carbon coat can affect the emitted intensities is due to the absorption of the primary beam electrons in the coating. This slowing down of the primary electrons results in an effective loss in energy of the incident electrons. For x-rays with a high overvoltage this reduction in primary beam energy is negligible, but for elements with an over voltage closer to 1.5 to 2 (for example Fe Ka at 10 KeV), this could affect the generated intensity calculation significantly.

## Appendix A: Timeline of Electron Microscopy and X-ray Microanalysis

1895 - X-rays discovered by Roentgen, produced by electron bombardment of inert gas in tubes; gas fluoresces and nearby photographic plates are exposed (X-rays' wavelength = 0.05 - 100 Å)

1898 - Starke in Berlin found backscatter intensity varies with Z

1909 - term "characteristic x-rays" first used by Barkla and Sadler but the physical origin of x-rays not clear and Kaye built an cathode ray tube with an ionization chamber to detect x-rays

1912 - Von Laue, Friedrich and Knipping confirmed that X-rays could be diffracted by crystals with lattice spacings of similar dimension

1913 - the Bohr model of the atom explained the characteristic x-ray spectra and Bragg obtained the first X-ray spectrum of Pt using an NaCl crystal (Bragg's Law:  $n \cdot \lambda = 2d \cdot \sin \theta$ )

1913 - Mosely found that there was a systematic variation of the wavelength of characteristic X-rays from various elements (wavelength inversely proportional to Z squared)

$$I = \frac{B}{(Z - C)^2}$$

where B and C are constants for each characteristic line family and Z is the atomic number.

1922 - Hadding used X-ray spectra to chemically analyze minerals

1923 - von Hevesy discovered Hf after noticing a gap at Z=72

late 1920's - in Germany, development of transmission electron microscopes, with first demonstration in 1932 of transmission electron microscopy by Ernst Ruska (belated Nobel prize for it in 1986) prototype build by Siemens & Halske Co but WWII prevented sale and use outside Germany

1930's - scanning coils added to TEM, producing STEM (image produced by secondary electrons emitted by specimen)

1940 - RCA sold first commercial TEM outside Germany

1942 - first use of SEM to examine surfaces of thick specimens at RCA Labs

1949 - Castaing built first electron microprobe for microchemical analysis (with crystal focusing wavelength dispersive spectrometer = WDS) for Ph.D at University of Paris, and developed the basic theory

1956 - commercial production of electron microprobe began (Cameca)

1965 - commercial production of SEM began

1968 - solid state EDS detectors developed

### *Useful References*

J. T. Armstrong, "Quantitative analysis of silicates and oxide minerals: Comparison of Monte-Carlo, ZAF and Phi-Rho-Z procedures," *Microbeam Analysis--1988*, p 239-246.

J. T. Armstrong, "Bence-Albee after 20 years: Review of the Accuracy of a-factor Correction Procedures for Oxide and Silicate Minerals," *Microbeam Analysis--1988*, p 469-476.

G. F. Bastin and H. J. M. Heijligers, "Quantitative Electron Probe Microanalysis of Carbon in Binary Carbides," Parts I and II, *X-Ray Spectr.* 15: 135-150, 1986

J. J. Donovan, D. A. Snyder and M. L. Rivers, "An Improved Interference Correction for Trace Element Analysis" *Microbeam Analysis*, 2: 23-28, 1993

J. J. Donovan and T. N. Tingle, "An Improved Mean Atomic Number Correction for Quantitative Microanalysis" in *Journal of Microscopy*, v. 2, 1, p. 1-7, 1996

J. I. Goldstein, D. E. Newbury, P. Echlin, D. C. Joy, C. Fiori, E. Lifshin, "Scanning Electron Microscopy and X-Ray Microanalysis", Plenum, New York, 1981

J. I. Goldstein, D. E. Newbury, P. Echlin, D. C. Joy, C. Fiori, E. Lifshin, "Scanning Electron Microscopy and X-Ray Microanalysis", 2nd Ed., Plenum, New York, 1992

K. F. J. Heinrich, "Mass Absorption Coefficients for Electron Probe Microanalysis" in *Proc. 11th ICXOM* 67: 1, 1982.

McQuire, A. V., Francis, C. A., Dyar, M. D., "Mineral standards for electron microprobe analysis of oxygen", *Am. Mineral.*, 77, 1992, p. 1087-1091.

Nielsen, C. H. and Sigurdsson, H., "Quantitative methods for electron microprobe analysis of sodium in natural and synthetic glasses", *Am. Mineral.*, 66, p. 547-552, 1981

J. L. Pouchou and F. M. A. Pichoir, "Determination of Mass Absorption Coefficients for Soft X-Rays by use of the Electron Microprobe" *Microbeam Analysis*, Ed. D. E. Newbury, San Francisco Press, 1988, p. 319-324.

S. J. B. Reed, *Electron Probe Analysis*, 2nd ed., Cambridge University Press, Cambridge, 1993

V. D. Scott and G. Love, "Quantitative Electron-Probe Microanalysis", Wiley & Sons, New York, 1983

K. G. Snetsinger, T. E. Bunch and K. Keil, "Electron Microprobe Analysis of Vanadium in the Presence of Titanium", *Am. Mineral.*, v. 53, (1968) p. 1770-1773